Adv. Sci. Res., 8, 39–44, 2012
www.adv-sci-res.net/8/39/2012/
doi:10.5194/asr-8-39-2012

Advances in Science & Research
Open Access Proceedings

Evening transitions of the atmospheric boundary layer: characterization, case studies and WRF simulations

M. Sastre[1], C. Yagüe[1], C. Román-Cascón[1], G. Maqueda[2], F. Salamanca[3], and S. Viana[4]

[1]Dept. de Geofísica y Meteorología, Universidad Complutense de Madrid, Spain
[2]Dept. de Astrofísica y Ciencias de la Atmósfera, Universidad Complutense de Madrid, Spain
[3]Lawrence Berkeley National Laboratory (LBNL), Berkeley (CA), USA
[4]Agencia Estatal de Meteorología (AEMET), Delegación Territorial de Cataluña, Barcelona, Spain

Correspondence to: M. Sastre (msastrem@fis.ucm.es)

Received: 20 October 2011 – Revised: 20 February 2012 – Accepted: 20 February 2012 – Published: 26 March 2012

Abstract. Micrometeorological observations from two months (July–August 2009) at the CIBA site (Northern Spanish plateau) have been used to evaluate the evolution of atmospheric stability and turbulence parameters along the evening transition to a Nocturnal Boundary Layer. Turbulent Kinetic Energy thresholds have been established to distinguish between diverse case studies. Three different types of transitions are found, whose distinctive characteristics are shown. Simulations with the Weather Research and Forecasting-Advanced Research WRF (WRF-ARW) mesoscale model of selected transitions, using three different PBL parameterizations, have been carried out for comparison with observed data. Depending on the atmospheric conditions, different PBL schemes appear to be advantageous over others in forecasting the transitions.

1 Introduction

The Planetary Boundary Layer (PBL) goes through different dynamical and thermal situations throughout a single day. Knowing how these changes are reached will be helpful to improve our understanding on various topics of the PBL, especially the transport of scalars – pollutants, water vapor, heat, etc. – in the lower troposphere and Earth-atmosphere exchanges and interactions (Baklanov et al., 2010). Having an enhanced comprehension of this subject will be very helpful for improvements on practical applications, such as atmospherically induced health alerts or agricultural topics.

This atmospheric layer is strongly influenced by the diurnal solar cycle, having a direct impact on surface heating and cooling and usually driven by turbulent processes. This fact leads us to look for the mechanisms that trigger the evolution from a convective PBL to a stable one at times around sunset. Changes that occur near the Earth's surface, namely the decay of the turbulence or the crossover of the sensible heat flux, mark the beginning of the evening transition from a certain time before sunset – which can vary between a few minutes and around one hour – Fernando et al. (2004). Here we study the following temporal interval: from two hours before sunset until four hours after sunset. In this way, conditions preceding the transition can be explored and the turbulence decay may also be studied from the time it starts. Additionally, the first hours of the night are investigated in order to explore how the different transitions can affect the development of the subsequent Nocturnal Boundary Layer (NBL).

The main aim of this work is to offer a framework for classifying turbulence decay in terms of TKE during the evening transition and to connect each class to some other phenomena in the NBL, like possible gravity waves or katabatic winds. To achieve this aim we studied some thermal and dynamical issues of the PBL. The study has two parts: the analysis of the experimental data and their comparison to WRF model simulations. Firstly, by using observations, it was investigated how rapidly the turbulence decays when the input solar radiation is reduced. In the second part, transitions corresponding to different situations were simulated with the WRF mesoscale model. The main goal of these simulations is to learn if a mesoscale model can adequately reproduce this turbulence decay. Furthermore, it can be interesting for future improvements in PBL transition modelling by Numerical Weather Prediction (NWP) models. It is also an objective to find relationships between characteristics of the transitions and different model settings, to find out which elements favour that the atmospheric behaviour is properly reflected by the model. Moreover, the comparison simulations-observations provides to us a wider point of view of the evening transition questions.

Published by Copernicus Publications.

2 Experimental data

Data employed for this study were obtained during July and August 2009 with some of the permanent instrumentation placed at a 10 m height mast in the Research Centre for the Lower Atmosphere – CIBA, for the Spanish acronym. These devices are sonic anemometers at 10 m height (working at a frequency of 20 Hz), temperature sensors at 1.5 (Z_1 level) and 10 m (Z_2 level) (1 Hz) and cup anemometers and vanes at 1.5 and 10 m (1 Hz). A picture of the mast can be found in Supplement 1. Additionally used, was a GRIMM 365 Monitor for measurements of particulate matter smaller than 1, 2.5 or 10 μm (PM_1, $PM_{2.5}$, PM_{10}, respectively) at the surface (1/6 Hz).

The CIBA site is located on the Northern Spanish plateau (41°49′ N, 4°56′ W), at 840 m above sea level and over a quite flat terrain. Nevertheless, two small slopes can be found: one in the NW-SE direction (1:6000) and the other one in the NE-SW direction (1:1660). These slopes should be taken into account for drainage flows. Some topographic maps of the location and the slopes scheme are provided in Supplement 1 (Viana, 2011). More details on the experimental site can be found by looking up Cuxart et al. (2000), and Yagüe et al. (2009) for the last instrumentation setup.

Five minute means were used for calculations of Turbulent Kinetic Energy ($TKE=\frac{1}{2}(\overline{u'^2}+\overline{v'^2}+\overline{w'^2})$, friction velocity ($U_* = \left[(\overline{u'w'})^2+(\overline{v'w'})^2\right]^{1/4}$) and vertical heat flux ($H = \rho c_p \overline{\theta' w'}$) from sonic anemometer records, considering the 3-D-wind components variances and covariances. Wind speed (U) and potential temperature (θ) were also evaluated in five minute means. The Bulk Richardson number (from Z_2 and Z_1 measurements) were used to look up stability and it is calculated as (Arya, 2001):

$$Ri_B = \frac{\frac{g}{T_o}\sqrt{Z_1 Z_2}\ln\left(\frac{Z_2}{Z_1}\right)\Delta\theta}{(\Delta U)^2}. \quad (1)$$

3 Model configuration

WRF-ARW numerical model version 3.3 was adopted for this study. This model is, at present, widely used for different kinds of simulations (Shin and Hong, 2011; García-Díez et al., 2012), both for operational and research goals, given that it can provide an important range of possibilities (i.e., different PBL or surface layer schemes and physical options). Here we briefly explain some aspects of the model configuration chosen to carry out our simulations. Four nested domains were configured, whose grids are, respectively, 27 km, 9 km, 3 km and 1 km, keeping its central point just on the CIBA coordinates. According to the number of grid points used for each domain, the smallest one is a 120 km-side square and the largest one has a side of 2700 km. For the vertical resolution, the model considers 50 eta levels, from which twenty-eight are located under the first kilometre, and also eight of them are under the first 100 m. The spin up used was 12 h and the time step was configured to be 90 s. For all the simulations the Noah Land Surface Model (LSM) was chosen, which is the unified NCEP/NCAR/AFWA scheme with soil temperature and moisture in four layers. Among the different options of PBL parameterizations, we used three: Mellor-Yamada-Janjic (MYJ) (Janjic, 1990), Mellor-Yamada-Nakanishi-Niino (MYNN) (Nakanishi et al., 2004) and Quasi-Normal-Scale-Elimination (QNSE) (Sukorianski et al., 2005). MYJ is basically the Eta operational scheme, which uses a one-dimensional prognostic TKE scheme allowing local vertical mixing. On the other hand, QNSE assumes a prognostic TKE equation, which is obtained from a theory for stably stratified regions, and its diffusivity allows for anisotropy. MYNN goes a bit further and can predict second order moments besides TKE. Every PBL parameterization uses a specific surface layer scheme: MYJ is run with the Monin-Obukhov (Janjic Eta) scheme while MYNN and QNSE use their own schemes (named also MYNN and QNSE). The long wave radiation (RRTM), short wave radiation (Dudhia) and microphysics package (WSM3) have been the same for all the simulations. Skamarock et al. (2008) can be checked for further details on the parameterizations and the model characteristics. Finally, the initial and boundary conditions were taken from NCEP-NCAR, whose horizontal resolution is 1° and the boundary conditions are forced every 6 h.

4 Results

4.1 Observational data

Thermodynamic and dynamic variables were studied for a six-hour interval, which takes sunset as the reference time ($t_{sunset} = 0$ h). With this normalization, the time interval studied went from −2 to +4 h. First of all, in order to get an overview of the transition, a brief analysis of mean values was done. You can find wind speed (at 1.5 and 10 m), temperature difference between 10 m and 1.5 m, particulate matter concentration, the Bulk Richardson number, Turbulent Kinetic Energy, friction velocity and vertical heat flux mean values in Table 1. They are shown separately in three time sub-intervals lasting two hours each, as far as the latter can be considered as different sub-periods dynamically and thermodynamically. We can generally see that stability increases as time goes on within the transition, with smaller values of turbulence parameters and a significant increase in particulate matter concentration, which does not diffuse to higher levels.

Turbulent Kinetic Energy, 1.5 m temperature, 10 m wind speed and temperature difference between 10 m and 1.5 m were calculated for the temporal interval previously mentioned. Figure 1 shows the 10 m Turbulent Kinetic Energy evolution of four evening transitions corresponding to the same week of August 2009. The same days are presented

Table 1. Mean values of wind speed, temperature difference between 10 and 1.5 m, the Bulk Richardson number, particle concentrations and turbulent parameters for the time ranges used at the CIBA site (July–August 2009). The sunset time is the reference: $t_{sunset} = 0$ h.

	$t = [-2,0]$ h	$t = [0,2]$ h	$t = [2,4]$ h
$U_{1.5}$ (m s^{-1})	2.74	2.10	2.08
U_{10} (m s^{-1})	4.35	3.74	3.72
$\Delta T_{10-1.5}$ (°C)	−0.27	1.17	1.01
Ri_B	−0.09	0.24	0.18
PM_1 (μg m^{-3})	3.02	4.76	6.90
$PM_{2.5}$ (μg m^{-3})	5.05	7.22	9.04
PM_{10} (μg m^{-3})	14.36	20.19	17.66
TKE (m^2 s^{-2})	0.94	0.55	0.42
U_* (m s^{-1})	0.36	0.26	0.24
H (W m^{-2})	19.02	−16.20	−17.56

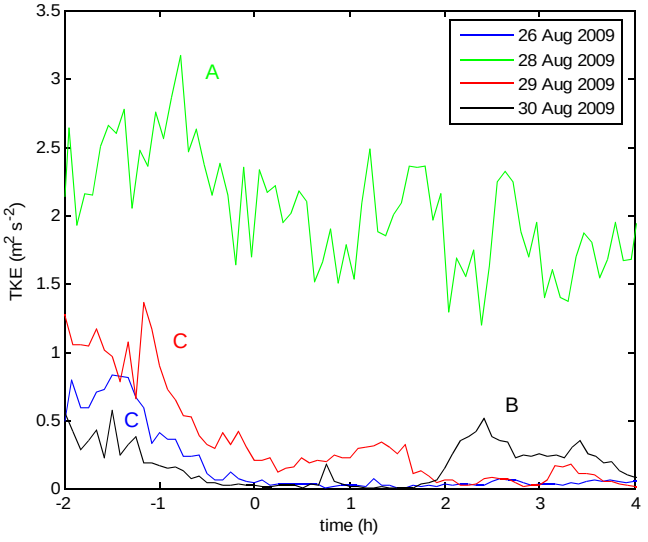

Figure 1. Observed TKE evolution at 10 m for different types of evening transitions (A, B, C). Times are normalized around sunset for each day ($t_{sunset} = 0$ h).

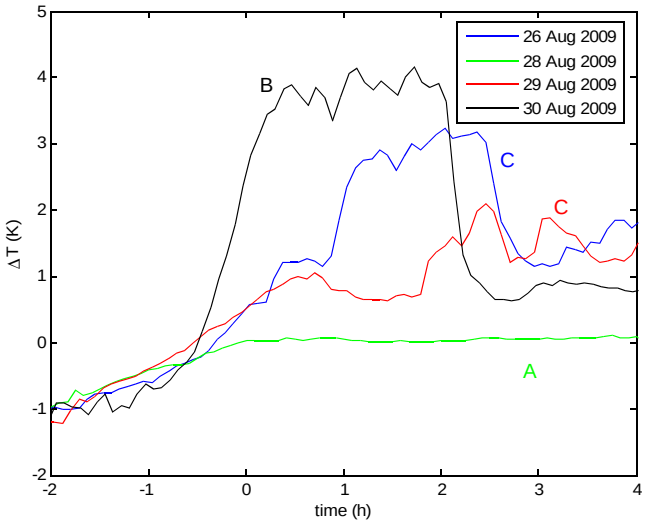

Figure 2. Observed 10–1.5 m temperature difference evolution for different types of evening transitions (A, B, C). Times are normalized around sunset for each day ($t_{sunset} = 0$ h).

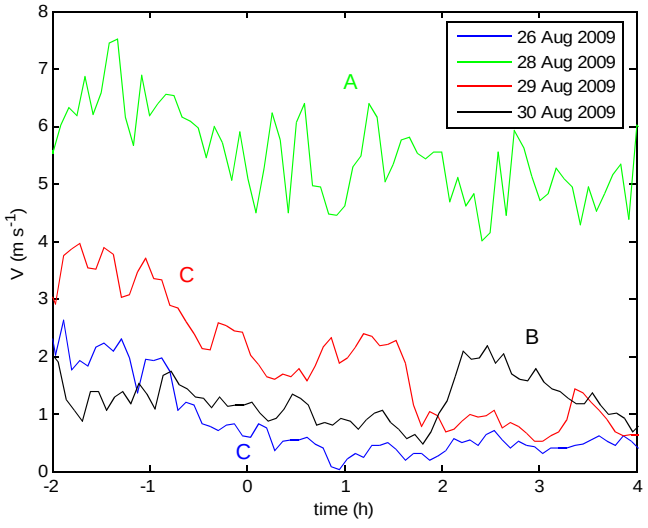

Figure 3. Observed 1.5 m wind evolution for different types of evening transitions (A, B, C). Times are normalized around sunset for each day ($t_{sunset} = 0$ h).

for the temperature difference (Fig. 2) and 1.5 m wind speed (Fig. 3). Actually, days plotted on Figs. 1–3 are examples of the three types of transitions we found during the two months of data analysed. First of all, we have the ones that are controlled by moderate to high synoptic winds (labelled in Figs. 1–3 with A). These were quite turbulent evenings, with no surface-based inversion temperature or a very weak one, and where TKE kept reaching values higher than 1.5 m^2 s^{-2}, sometimes not very different from diurnal ones. On the other hand, there were some transitions with very small values of TKE (<0.5 m^2 s^{-2}) and wind speed before sunset, so that an early and strong surface-based inversion developed (B). This strong stability is very likely to the occurrence of katabatic winds, which can erode the stability (see increase of TKE two hours after sunset) and are sometimes related to the generation of gravity waves (Viana et al., 2010). Finally, a third group of transitions would consist of those ones with light to moderate winds before sunset, developing a soft and continuous inversion during the night without important katabatic events (C). TKE values between 0.5 and 1.5 m^2 s^{-2} were characteristic of the latter group. The two months of data collected for this work show that in this period the most common transitions were type C (39 %), followed by type B (32 %), while type A (18 %) was the least frequent to occur. There are still some cases (11 %) that cannot be easily classified as any of these three types.

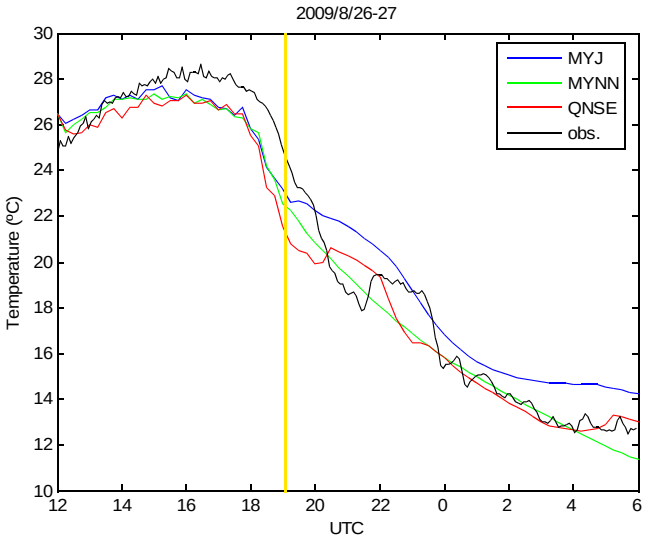

Figure 4. Simulations of 2 m-air temperature and comparison with 5-min averaged observations for the 26–27 August 2009 transition (type C).

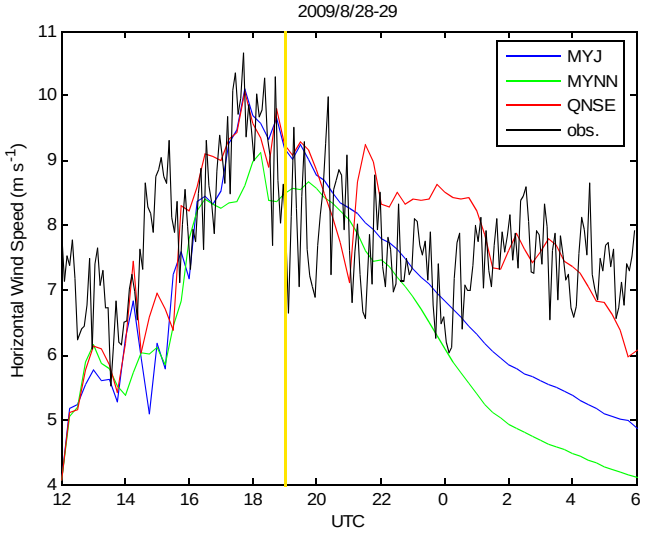

Figure 5. Simulated and observed (5-min averaged) wind speed at 10 m for 28–29 August transition (type A).

4.2 WRF simulations

Wind speed, temperature and friction velocity were simulated for the evening transitions of certain days which are representative of different situations, for comparison with observed data.

The selected PBL parameterizations tend to smooth the observed behaviour of the magnitudes represented. Temperature was, as a whole, well-simulated both qualitatively and quantitatively and with a correct timing by the three parameterizations, although high frequency peaks were not captured

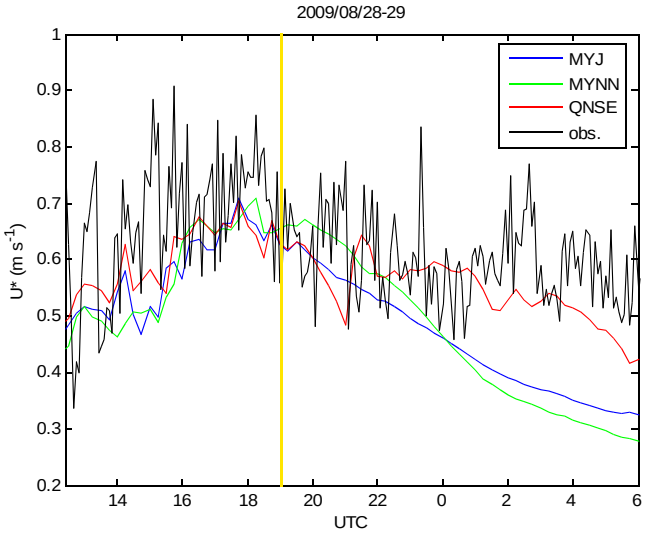

Figure 6. Simulated and observed (5-min averaged) friction velocity for 28–29 August transition (type A).

(see day 26 August, Fig. 4). In Fig. 4 it is remarkable that during the temperature decay there was an observed upturn, which seems to be captured only by QNSE parameterization, although one or two hours in advance. Windy transitions (type A) are usually better simulated by QNSE, while MYJ and MYNN fail to reproduce the beginning of the night, providing a continuous decay of the wind and friction velocity when it does not really happen (see wind speed and friction velocity for day 28 August, Figs. 5 and 6). Regarding transitions with early-developed inversions and katabatic winds, (type B) not very good agreement between experimental data and simulations has been had at times for big changes in the PBL structure (see friction velocity for day 30 August, Fig. 7). Nevertheless, the observed decay and later fast rise might have been simulated by QNSE and MYJ, but a couple of hours before it happened, and reaching significantly smaller maximum and minimum values than the observed ones. For type C, QNSE gave better results when the inversion was already developed, probably because QNSE is especially designed for stable situations.

To evaluate simulations a bit more deeply than from a visual inspection, two parameters were calculated to compare the model's outputs with observations: bias and root-mean-square error (RMSE), which are respectively defined as:

$$\mathrm{BIAS}=\frac{1}{N}\sum_{i=1}^{N}(\phi_{\mathrm{m}_i}-\phi_{\mathrm{o}_i}) \tag{2}$$

$$\mathrm{RMSE}=\left[\frac{1}{N}\sum_{i=1}^{N}(\phi_{\mathrm{m}_i}-\phi_{\mathrm{o}_i})^2\right]^{1/2} \tag{3}$$

where "N" is the number of data considered to calculations, "ϕ" indicates the variable being evaluated and de sub-indexes

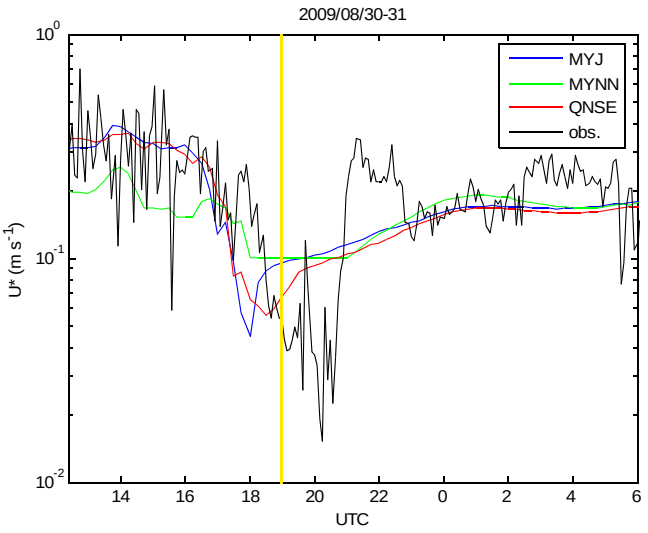

Figure 7. Simulated and observed (5-min averaged) friction velocity for the 30–31 August 2009 transition (type B).

"m" and "o" refer to modelled or observed data, respectively. A table of bias and RMSE values associated to the data for Figs. 4 to 7 can be found in Supplement 2.

According to the bias, the friction velocity is usually underestimated by the parameterizations – opposite to the overestimation that is frequently seen –, except for one particular situation: in the interval of two hours after sunset during day 30 August, which is type B.

MYNN parameterization is most of the time the one that obtains lower values of RMSE. However, although QNSE is rarely the best one at RMSE, sometimes it is the only one that captures some particular events, such as a short climb in temperature during a descending trend.

5 Conclusions

Three different types of observed PBL evening transitions were found for the summer 2009 at CIBA and some TKE thresholds may be used to classify them: the windy and with nearly no temperature inversion ones have TKE $> 1.5\,m^2\,s^{-2}$; the ones with early strong inversions (B) correspond to TKE $< 0.5\,m^2\,s^{-2}$ and intermediate cases (C) take place when $0.5 <$ TKE $< 1.5\,m^2\,s^{-2}$.

Considering WRF model simulations, we found no clear evidence to conclude which one of the three PBL parameterizations tested is the best at simulating evening transitions, as far as all the three are able to reproduce the observed behaviour in certain circumstances. QNSE seems to simulate some events while the other ones do not, although not with the correct timing or intensity. Further research is required in order to improve the simulation results, especially for difficult events such as katabatic winds. Moreover, a new theoretical framework might be necessary, as suggested by Nadeau et al. (2011), to describe the TKE during the evening transition when winds are very light and the mechanical turbulence production decreases.

Supplementary material related to this article is available online at: http://www.adv-sci-res.net/8/39/2012/asr-8-39-2012-supplement.zip.

Acknowledgements. The authors wish to thank Javier Peláez (CIBA) for his technical support and help as well as J. L. Casanova, Director of the CIBA. We are also very grateful to the editor and two anonymous referees for their constructive suggestions, which helped to improve this paper. This research has been funded by the Spanish Ministry of Science and Innovation (projects CGL 2006-12474-C03-03 and CGL2009-12797-C03-03). The GR58/08 program (supported by BSCH and UCM) has also partially financed this work through the Research Group "Micrometeorology and Climate Variability" (No 910437). M. Sastre is supported by a FPI-UCM fellowship (reference BE45/10).

Edited by: G.-J. Steeneveld
Reviewed by: two anonymous referees

The publication of this article is sponsored by the European Meteorological Society.

References

Arya, S. P. S.: Introduction to Micrometeorology, 2nd Edn., International Geophysics Series, Academic Press, London, 307 pp., 2001.

Baklanov, A., Grisogono, B., Bornstein, R., Mahrt, L., Zilitinkevich, S., Taylor, P., Larsen, S., Rotach, M., and Fernando, H. J. S.: On the nature, theory, and modelling of atmospheric planetary boundary layers, B. Am. Meteorol. Soc., 92, 123–128, 2010.

Cuxart, J., Yagüe, C., Morales, G., Terradellas, E., Orbe, J., Calvo, J., Fernández, A., Soler, M. R., Infante, C., Buenestado, P., Espinalt, A., Joergensen, H. E., Rees, J. M., Vilà, J., Redondo, J. M., Cantalapiedra, I. R., and Conangla, L.: Stable Atmospheric Boundary-Layer Experiment in Spain (SABLES 98): a report, Bound.-Lay. Meteorol., 96, 337–370, 2000.

Fernando, H. J. S., Princevac, M., Pardyjak, E. R., and Dato, A.: The decay of convective turbulence during evening transition period. Paper 10.3, 11th Conf. on Mountain Meteorology and MAP Meeting, Bartlett, NH, Amer. Meteor. Soc., 4 pp., 2004.

García-Díez, M., Fernández, J., Fita, L., and Yagüe, C.: WRF sensitivity to PBL parametrizations in Europe over an annual cycle, Q. J. Roy. Meteor. Soc., under review, 2012.

Janjic, Z. A.: The step-mountain coordinate: physics package, Mon. Weather Rev., 118, 1429–1443, 1990.

Nadeau, D. F., Pardyjak, E. R., Higgins, C. W., Fernando, H. J. S., and Parlange, M. B.: A simple model for the afternoon and early evening decay of convective turbulence over different land surfaces, Bound.-Lay. Meteorol., 141, 301–324, 2011.

Nakanishi, M. and Niino, H.: An improved Mellor-Yamada level-3 model with condensation physics: its design and verification, Bound.-Lay. Meteorol., 112, 1–31, 2004.

Shin, H. H. and Hong, S.-Y.: Intercomparison of Planetary Boundary-Layer parametrizations in the WRF model for a single day from CASES-99, Bound.-Lay. Meteorol., 139, 261–281, 2011.

Skamarock, W. C., Klemp, J. B., Dudhia, J., Gill, D. O., Barker, D. M., Duda, M. G., Huang, X.-Y., Wang, W., and Powers, J. G.: A description of the advanced research WRF version 3. NCAR Technical note, NCAR/TN-475+STR, 113 pp., 2008.

Sukorianski, S., Galperin, B., and Perov, V.: Application of a new spectral theory of stable stratified turbulence to the atmospheric boundary layer over sea ice, Bound.-Lay. Meteorol., 117, 231–257, 2005.

Viana, S.: Estudio de los procesos físicos que tienen lugar en la capa límite atmosférica nocturna a partir de campañas experimentales de campo, Ph.D. thesis, Faculty of Physical Sciences, University Complutense of Madrid, Spain, 238 pp., 2011.

Viana, S., Terradellas, E., and Yagüe, C.: Analysis of gravity waves generated at the top of a drainage flow, J. Atmos. Sci., 67, 3949–3966, 2010.

Yagüe, C., Sastre, M., Maqueda, G., Viana, S., Ramos, D., Vindel, J. M., and Morales, G.: CIBA2008, an experimental campaign on the atmospheric boundary layer: preliminary nocturnal results, Física de la Tierra, 21, 13–26, 2009.